SUPPORTING INFORMATION

Understanding the Role of Molecular Diffusion and Catalytic Selectivity in Liquid-Phase Beckmann Rearrangement

Matthew E. Potter,[a] Alexander J. O'Malley,[b,c] Stephanie Chapman,[a] Julija Kezina,[a,d] Stephanie H. Newland,[a] Ian P. Silverwood,[c,e] Sanghamitra Mukhopadhyay,[e] Marina Carravetta,[a] Thomas M. Mezza,[f] Stewart F. Parker,[c,e] C. Richard A. Catlow[b,c,g] and Robert Raja[a,c]*

a. School of Chemistry, University of Southampton, University Road, Southampton, SO17 1BJ, UK.

b. Department of Chemistry, University College London, 20 Gordon Street, London WC1H 0AJ, UK.

c. UK Catalysis Hub, Research Complex at Harwell, Science and Technology Facilities Council Rutherford Appleton Laboratory, Harwell Science and Innovation Campus, Oxon OX11 0QX, UK.

d. Analytical Sciences and Development, GSK, Medicines Research Centre, Gunnels Wood Road, Stevenage, Hertford-shire, SG1 2NY, UK.

e. ISIS Pulsed Neutron and Muon Facility, Science and Technology Facilities Council Rutherford Appleton Laboratory, Harwell Science and Innovation Campus, Oxon OX11 0QX, UK.

f. UOP LLC, A Honeywell Company, 25 East Algonquin Road, Des Plaines, IL 60017, USA.

g. Cardiff Catalysis Institute, School of Chemistry, Cardiff University, UK.

*Corresponding author: Robert Raja, R.Raja@soton.ac.uk

CONTENTS

Experimental details

Synthesis details

Full details of the SAPO-37 synthesis are described in reference 1. *Pseudo*-Boehmite was added to the mixture of phosphoric acid (85 % in water) and water and then stirred for 7 h. Fumed silica was slowly added to a stirred solution of TPAOH and TMAOH · $5H_2O$, was stirred for 2 h and added to the first mixture. The gel was stirred for 68 h before it was transferred to a Teflon-lined tube, sealed inside a stainless-steel autoclave that was put in an oven at 200 °C for 24 h. The contents were then centrifuged, filtered and washed with deionized water. The material was dried overnight at room temperature. Before catalysis the white solid was calcined at 550 °C for 8 h and stored under inert atmosphere. ZSM-5 and Zeolite-Y samples were purchased from Zeolyst, with Si/Al ratios of 30.

Characterisation protocols

The characterisation was performed on a freshly calcined virgin SAPO-37 sample (unless specifically stated otherwise), that was vacuum dried at around 120 ^{o}C to remove moisture, owing to prior art showing that SAPO-37 is moisture sensitive.

Powder X-ray diffraction patterns were obtained using a Siemens D5000 diffractometer using Cu $K_{\alpha 1}$ radiation, whereby λ = 1.54056 Å. Rietveld refinement was performed using the appropriate space group. This was performed on freshly calcined sample.

BET surface area measurements were performed using a Micromeritics Gemini 2375 surface area analyser and prepared using flow gas preparation. Samples were degassed at 120 ^{o}C under vacuum for 12 hours prior to this.

A Perkin-Elmer Optimum 3000 DV was used for ICP analyses with calcined samples prepared and fully digested in 10 mL of deionised water and 10 mL of ACS Plus Certified H_2SO_4 (Fisher Scientific). Solutions of standard concentrations were used for calibration.

Scanning electron microscopy images were obtained using a JOEL-JSM5910 microscope with an accelerating voltage of 0.3-30 kV. The samples were prepared by carbon coating.

All the ^{29}Si and ^{31}P NMR measurements were performed on a Chemagnetics Infinity 400 spectrometer on a 4 mm MAS double-resonance APEX probe. For all samples, approximately 100 mg of material was quickly transferred into a thin wall zirconium oxide rotor and then spun at 8 kHz in air, for bearing, drive and purge. ^{31}P NMR data were acquired with direct acquisition (4 scans and 120 s delay between scans). ^{29}Si NMR data for all 1D experiments were performed using cross-polarization and SPINAL64[2] decoupling. Typical spectra were acquired with 8192 scans and 2 s between scans.

The ^{27}Al measurements were performed at 14.1 T on a wide bore Bruker Avance II spectrometer using a 2.5 mm double resonance probe and a spinning frequency of 25 kHz. ^{27}Al NMR experiments were performed using direct acquisition (128 scans with a pulse delay of 2 s between scans). Two dimensional 3QMAS experiments (Figure 5 in main paper) were performed using the z-filtered method.[3] The SAPO-37 3QMAS spectrum was acquired with 220 t_1 increments of 20 μs, 360 scans

and a pulse delay of 1s. The 3QMAS spectra for zeolite Y and ZMS-5 were acquired with 360 t_1 increments of 10μs, 840 scans and a pulse delay of 0.15 s. The chemical shift axes in the ^{27}Al, ^{31}P and ^{29}Si spectra were referenced using 1M $AlCl_3$ aqueous solution (0 ppm), 85 % H_3PO_4 (0 ppm) and silicon rubber (–22.42 ppm) respectively. The NMR data were processed using matNMR.[4] All NMR samples were dried at 120 ^oC under vacuum for 12 hours prior to analysis, unless stated otherwise.

Low temperature CO FT-IR experiments were performed in a custom designed IR flow cell that allowed for sample heating and cryogenic cooling. Freshly calcined samples were ground and pressed into 13 mm diameter self-supporting pellets (~8 mg cm^{-2}) and heated at 10 ^oC min^{-1} to 550 ^oC in a mixture of 20 % O_2 in N_2 [Matheson UHP grade further purified using a P400 air purifier(VICI)] and held for 1 h. The flow was then switched to helium [Matheson UHP grade further purified using a P-100 helium purifier(VICI) and an indicating OMI-1 purifier(Supelco)] and held for an additional hour. The system was then cooled to ~ -175^oC and a spectrum recorded. Nine 0.02 cm^3 injections of CO (Matheson research purity) were added to the system followed by a final injection of 0.20 cm^3. After each injection, the system was equilibrated for 3 min and a spectrum recorded. All spectra were collected on a Nicolet Nexus 870 FTIR spectrometer using a cooled MCT detector. Each spectrum was obtained by co-adding 128 scans at a resolution of 2 cm^{-1}. All spectral processing was done using the GRAMS/AI 9 software (Thermo Scientific). All spectra are normalized to a 10 mg pellet weight. Difference spectra were obtained by subtracting the spectrum of the sample before adsorption of the probe molecule.

Collidine-probed FT-IR experiments were performed as follows. Freshly calcined samples were ground and pressed into 13 mm diameter self-supporting pellets (~ 8 mg cm^{-2}) and heated at 10 ^oC min^{-1} to 550 ^oC in a mixture of 20 % O_2 in N_2 [Matheson UHP grade further purified using a P400 air purifier(VICI)] and held for 2 h. The system was then cooled to 30 ^oC and a spectrum recorded. The sample was equilibrated with collidine (helium saturated with collidine vapour at 7 ^oC) for 1 h at 150 ^oC. Stepwise desorption of collidine was done at 150, 300 and 450 ^oC. After 1 h hold at each desorption temperature, the sample was cooled to room temperature and a spectrum recorded. All spectra were collected on a Nicolet Nexus 870 FTIR spectrometer using a cooled MCT detector. Each spectrum was obtained by co-adding 128 scans at a resolution of 2 cm^{-1}. All spectral processing was performed using the GRAMS/AI 9 software (Thermo Scientific). All spectra were normalized to a 10 mg pellet weight. Difference spectra were obtained by subtracting the spectrum of the sample before adsorption of the probe molecule.

All TPD measurements were performed on a custom-built system using TCD detectors to monitor ammonia concentration. Freshly calcined samples were pre-treated by heating at 10 ^oC min^{-1} to 550 ^oC in a 20 % O_2/ helium mixture [Matheson UHP grade passed through a Drierite/molecular sieve gas purifier (Alltech Associates)] and held for 2 h. The samples were exposed to ammonia and allowed to equilibrate at 150 ^oC for 8 h. Desorption was performed in flowing helium [Matheson UHP grade further purified with an Oxy-Trap (Alltech Associates) and an indicating OMI-1 purifier (Supelco)] at 10 ^oC min^{-1} to 600 ^oC and held for 40 minutes at 600 ^oC.

Catalytic procedure

The liquid-phase Beckmann rearrangement of cyclohexanone oxime was carried out with 0.9 mmol cyclohexanone oxime, using a 9:1 molar ratio of oxime:catalyst in 20 mL of anhydrous benzonitrile (> 99% purity; Aldrich) in a stirred glass reactor at 130 ^{o}C. Samples were taken at appropriate intervals. Recycle experiments were performed by filtering the reaction mixture, washing the catalyst with warm, anhydrous benzonitrile and recalcining the sample at 550 ^{o}C for 8 hours, storing under dry, inert conditions between catalysis cycles.

All samples were analysed on a Perkin Elmer Clarus 480 gas chromatograph with a flame ionization detector (FID), fitted with an autosampler, employing a HP1 cross linked methylsiloxane (30 m x 0.32 mm x 1 µm film thickness) column. Mass-balance was determined for all samples using chlorobenzene as an internal standard. Products were identified against authenticated standards and quantified by calibration to obtain response factors (R_F) against the known internal standard.

Start temperature 120 ^{o}C, hold 2 min, ramp at 15 ^{o}C min^{-1} up to 220 ^{o}C, hold for 5 min at 220 ^{o}C. The method is 13 minutes and 40 seconds long in total. The benzonitrile solvent peak was a large peak at 3.5 min, the cyclohexanone oxime was at 4.0 min, ε-caprolactam peak was at 5.8 min, and the by-product is at 6.6 min. The injector port was set to 220 ^{o}C, the detector was set to 250 ^{o}C. The carrier pressure (helium) was at 14 psig. The method was given 1 min to equilibrate before injection. Typically 5 µl of centrifuged sample was injected.

The response factors were used to calculate the moles of cyclohexanone oxime, ε-caprolactam and by-products (response factor assumed to be 1.00). The conversion was calculated as:

Conversion = 100 x (initial moles of oxime – moles of oxime detected) / initial moles of oxime

Selectivity = 100 x (moles of caprolactam) / moles of products detected

Introduction to QENS theory

The following has been adapted from reference 27 of the main article, a more comprehensive discussion of the appropriate theory of the technique can be found therein. Incoherent neutron scattering is ideal for studying hydrocarbon diffusion in zeolites,[5] as hydrogen has the largest incoherent scattering cross section.

Molecular motions can be described by Fick's law;

$$\frac{\partial p(\mathbf{r},t)}{\partial t} = D_{\mathrm{s}} \nabla^2 p(\mathbf{r},t)$$

with *p(r,t)* being the probability of finding an atom at position *r* at time *t*, and D_s being the self-diffusion coefficient of the molecule. *p(**r**,t)* is solved using the self part of the van Hove correlation function:

$$G_{\mathrm{s},i}(\mathbf{r},t) = \langle \delta[\mathbf{r} - \mathbf{r}_{\ell i}(t) + \mathbf{r}_{\ell i}(0)] \rangle$$

which is a probability density that a molecule *i* will be displaced by a vector r within time *t*

at equilibrium. The incoherent scattering function S(Q,ω) is the four dimensional Fourier transform of the van Hove correlation function

$$S(\mathbf{Q},\omega) = \frac{1}{2\pi}\int \mathrm{d}t \exp(-\mathrm{i}\omega t)\int \mathrm{d}\mathbf{r}\exp(\mathrm{i}\mathbf{Q}\cdot\mathbf{r})G(\mathbf{r},t)$$

The incoherent translational scattering function for a molecule following Fick's law or jump diffusion can be described by a Lorentzian function:

$$S(\mathbf{Q},\omega) = \frac{1}{\pi}\frac{D_s Q^2}{\omega^2 + (D_s Q^2)^2}$$

where $\hbar Q$ describes the neutron momentum transfer and $\hbar\omega$ is the neutron energy transfer. For isotropic diffusion, if the momentum transfer is sufficiently small, *i.e.* diffusion over large distances, the half-width at half-maximum (HWHM) of the Lorentzian is D_sQ^2 where D_s is the self-diffusion coefficient and a plot of the HWHM of the Lorentzian component as a function of Q should give a D_sQ^2 dependence.

At smaller distances (larger Q values), there is usually a deviation from the linear relation between

$$\Delta\omega(Q) = D_s Q^2$$

$\Delta\omega$ and Q^2. The error in the diffusion coefficient is then calculated from the uncertainty of this gradient, as done for cyclohexanone oxime in HY. If one considers only isotropic systems, the scattering function will always be a Lorentzian function, but the width (HWHM) of the energy spectra will differ from the simple DQ^2 behaviour. For example, in the case of a molecule jumping from site to site in the zeolite structure, these movements are connected to the observed $S(Q,\omega)$ by a number of different models. The models contain as parameters the characteristic lengths and times of the elementary steps.

The model used in this work was derived by Chudley and Elliot;[6,7] the jump distance d is a constant and the HWHM is given by:

$$\Delta\omega(Q) = \frac{1}{\tau}\left(1 - \frac{\sin(Qd)}{Qd}\right)$$

where τ is the residence time of the molecule on a given site.

The diffusion coefficient is then extrapolated using:

$$\boldsymbol{D_s = \frac{d^2}{6t}}$$

As outlined in reference 27 of the main article. The error in the D_s is then calculated from the uncertainty in both the residence time and the jump distance. We note that in our study the errors in our approximated D_s of cyclohexanone oxime in SAPO-37 from this model, are an order of magnitude higher than those calculated directly from the Fickian model used in HY. This illustrates that while the diffusivities are similar in magnitude when errors are considered, due caution must be exercised when making direct comparison of the measured D_s values, given the differing diffusion mechanisms that operate within the two catalysts.

Further characterisation data

Powder XRD patterns

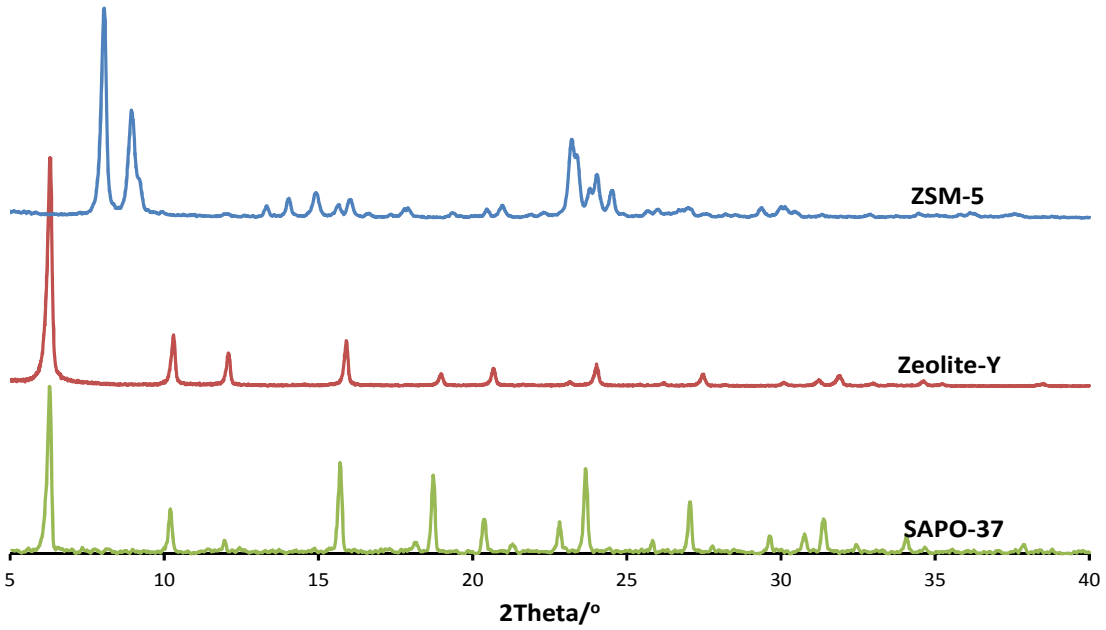

Figure S1: Powder XRD patterns of ZSM-5 (top), Zeolite-Y (middle) and SAPO-37 (bottom) showing phase pure MFI, FAU and FAU topologies respectively.

KI was used as a standard to measure relative crystallinity by scanning a physical mixture of 50% KI and 50% zeotype. The intensity of the 25.2° KI peak was used to normalise the peak areas of the 6.3° FAU peaks. This resulted in Zeolite-Y having a relative crystallinity of 1.42, compared to KI and SAPO-37 having a relative crystallinity of 1.34, compared to KI. This shows that the crystallinity of SAPO-37 and Zeolite-Y is in excellent agreement.

Scanning electron microscopy (SEM) images

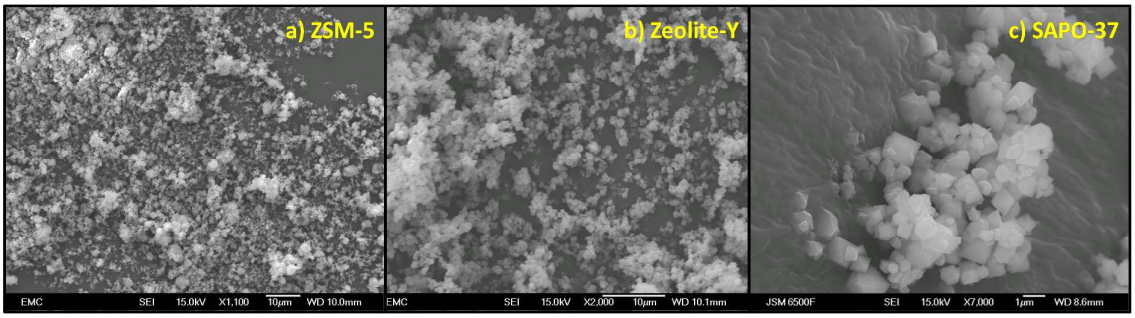

Figure S2: SEM images of a) ZSM-5 showing a range of crystallite sizes due to particle agglomeration, b) Zeolite-Y showing cubic particles around 1 µm in size and c) SAPO-37 also showing cubic particles around 1 µm in size.

Summary of textural data

Table S1: Contrasting the physical characteristics of the different catalysts.

System	Powder XRD					Metal content/wt%			Micropore volume/$cm^3\ g^{-1}$	Surface area/$m^2\ g^{-1}$
	Space group	a/Å	b/Å	c/Å	Crystallite size/nm	Si	Al	P		
ZSM-5	Pnma	20.0	19.8	13.3	45.2	43.7	2.97	-	0.014	312
Zeolite-Y	Fd-3m	24.3	24.3	24.3	48.1	43.8	2.87	-	0.021	644
SAPO-37	Fd-3m	24.4	24.4	24.4	52.4	2.95	23.5	20.8	0.010	588

QENS data

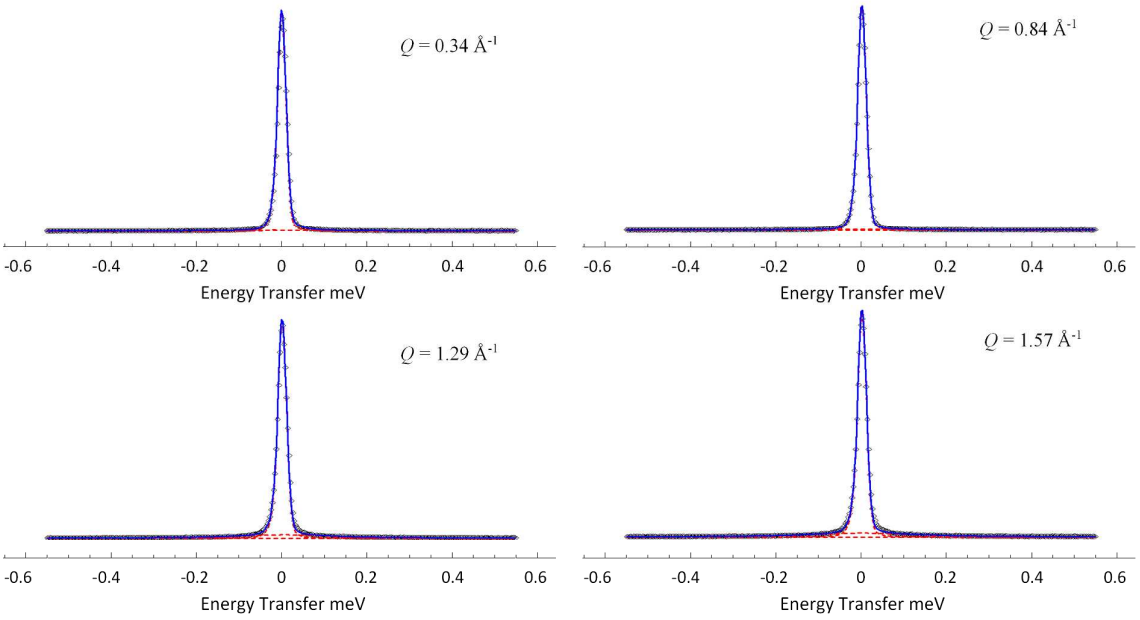

Figure S3: QENS spectra obtained for cyclohexanone oxime diffusing in ZSM-5 at 4 different Q-values at 373 K (blue), fitted using a linear combination of Lorentzian functions (red). Units of Δω in meV on the x-axis, the y-axis is in arbitrary units.

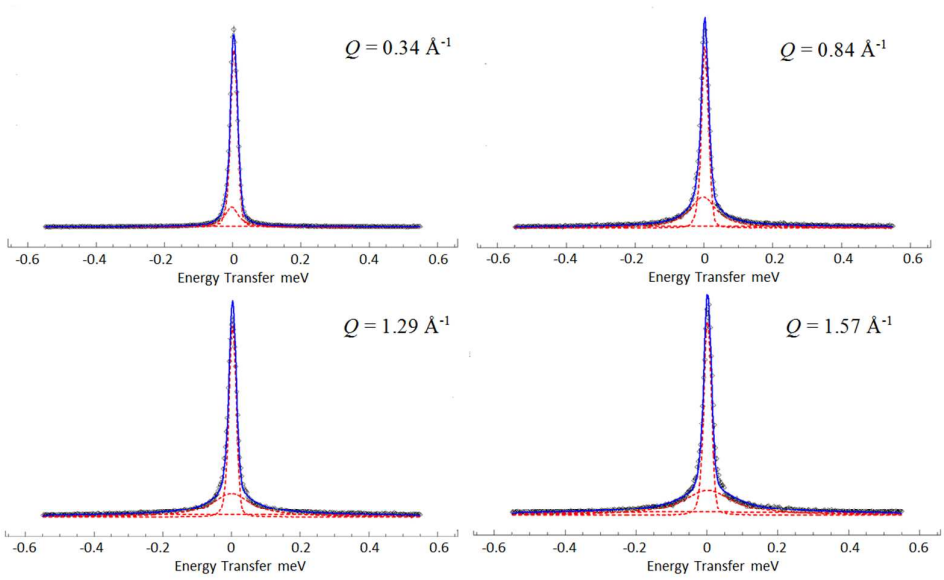

Figure S4: QENS spectra obtained for cyclohexanone oxime diffusing in Zeolite-Y at four different *Q* values at 373 K, showing the total fit (blue) and constituent resolution, Lorentzian and flat background functions (red).

1D ^{31}P MAS NMR spectrum

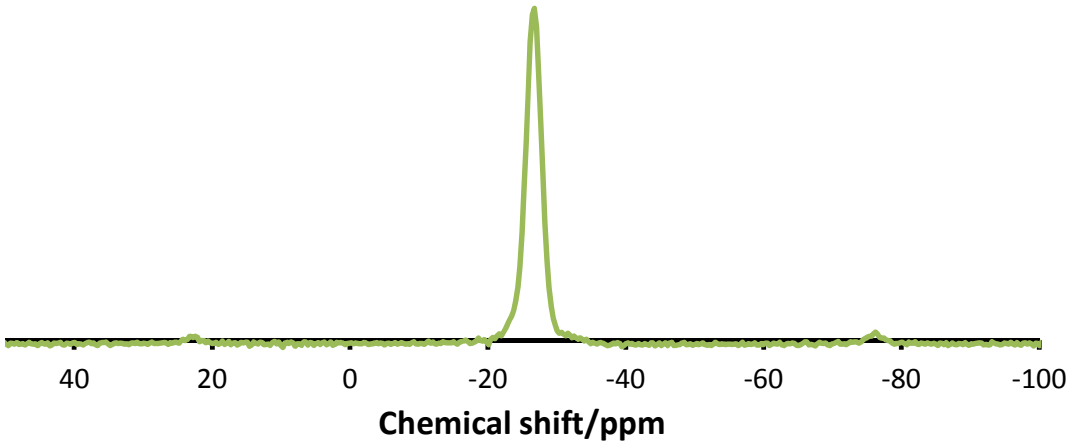

Figure S5: ^{31}P MAS NMR of SAPO-37 with peak centred at -26.7 ppm, assigned to $P(OAl)_4$.

1D ^{27}Al NMR spectrum

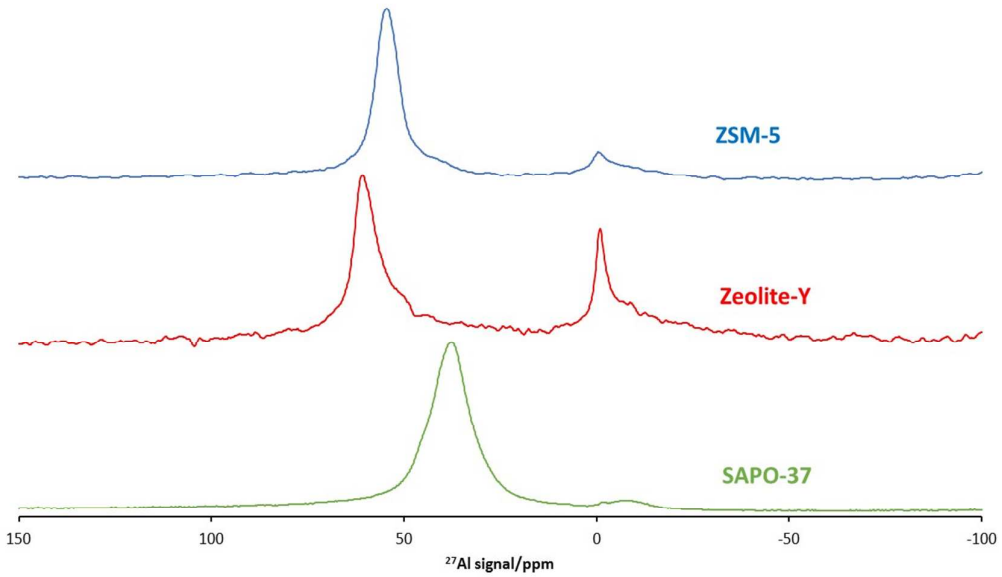

Figure S6: 1D ^{27}Al MAS NMR spectra of ZSM-5 (top), Zeolite-Y (middle) and SAPO-37 (bottom). The zeolite species show primary peaks between 54 – 62 ppm attributed to $Si(OAl)_4$, with peaks near 0 ppm attributed to extra–framework octahedral aluminium species. SAPO-37 shows just one broad signal at 38 ppm, attributed to $Al(OP)_4$ and $Al(OP)_3(OSi)$ species.

Table S2: NMR parameters from ^{27}Al measurements on SAPO-37, as estimated from peak position in the MQMAS experiments.

System	δ_{iso} (ppm)	P_Q (MHz)
SAPO-37, main site	38.1(5)	2.3(3)
SAPO-37	46.6(5)	4.9(4)
SAPO-37, surface defect	41.8(5)	4.4(2)
Zeolite-Y, main site	61.2(5)	3.0(3)
Zeolite-Y	61.9(5)	2.0(2)
Zeolite-Y	-1.0(3)	0.0(1)
ZSM-5, main site	55.1(5)	1.1(2)
ZSM-5	58.4(5)	5.1(4)
ZSM-5	-0.5(3)	0.0(1)

1D ^{29}Si MAS NMR spectrum

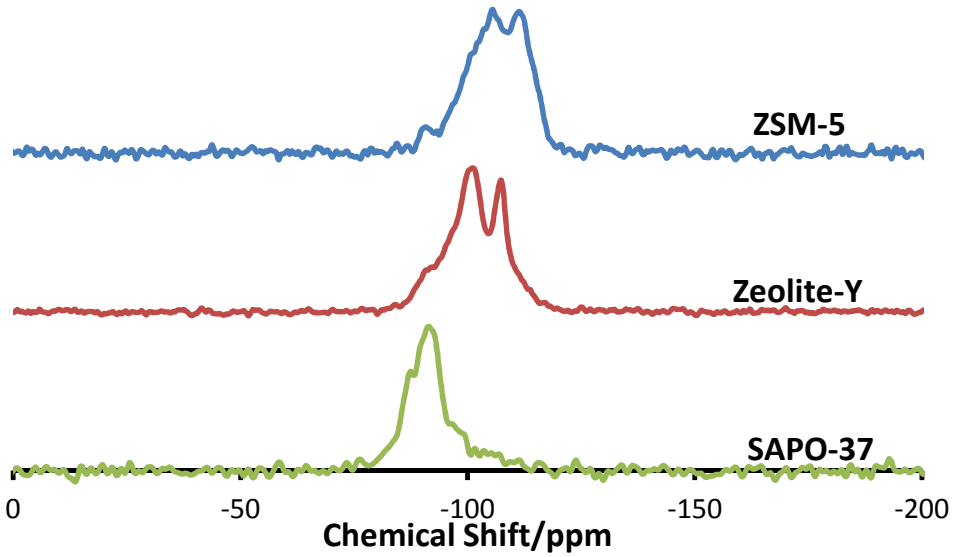

Figure S7: 1D ^{29}Si MAS NMR spectra of ZSM-5 (top), Zeolite-Y (middle) and SAPO-37 (bottom). The zeolite species show two peaks, one between -111 to -106 ppm, attributed to $Si(OSi)_4$, the other signal is between -105 to -101 ppm, attributed to $Si(OSi)_3(OAl)$ and $Si(OSi)_3(OH)$ species. SAPO-37 shows just one peak, centred at -91 ppm, attributed to $Si(OAl)_4$, confirming framework substitution.

NH_3-TPD data

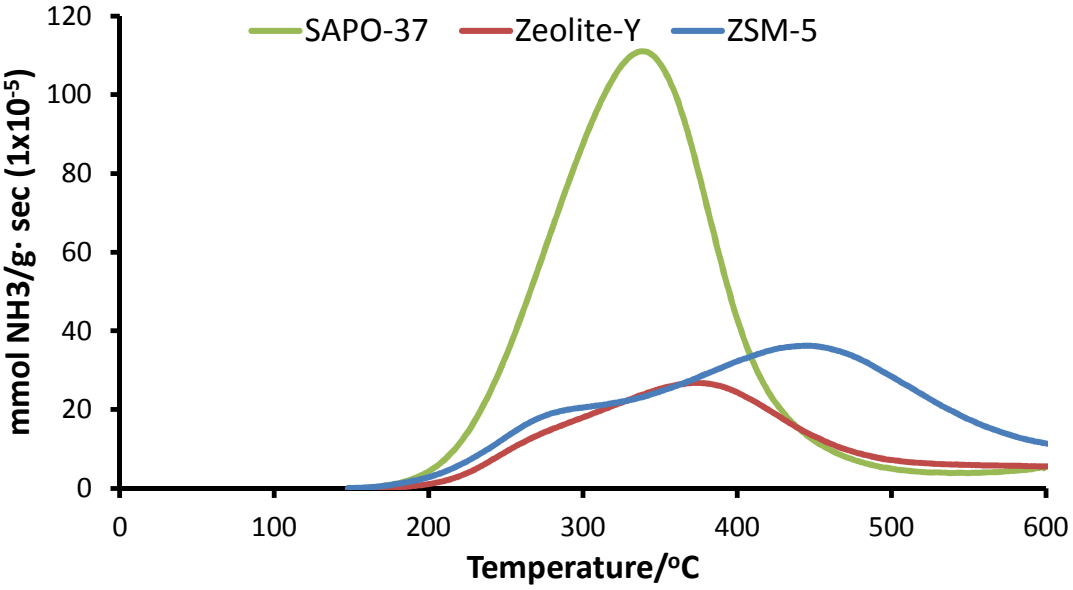

Figure S8: NH_3-TPD data showing SAPO-37 (green), Zeolite-Y (red) and ZSM-5 (blue). The zeolite samples show two signals, one at 270 °C corresponding to defect Si-OH species. Zeolite-Y shows a second peak at 370 °C and ZSM-5 shows a second peak at 440 °C, both correspond to Si-OH-Al groups. Interestingly, SAPO-37 shows a single broad peak at 340 °C, corresponding to isolated Brønsted acid sites.

Table S3: Integrated peak areas for NH_3-TPD data.

System	Integrated peak area over specific temperature range						Peak
	150-200	200-300	300-400	400-500	500-600	Total	maximum/°C
SAPO-37	0.000	0.237	0.563	0.094	0.033	0.927	340
Zeolite-Y	0.001	0.057	0.146	0.085	0.037	0.326	370
ZSM-5	0.003	0.078	0.154	0.206	0.111	0.552	440

FT-IR spectra of the hydroxyl region

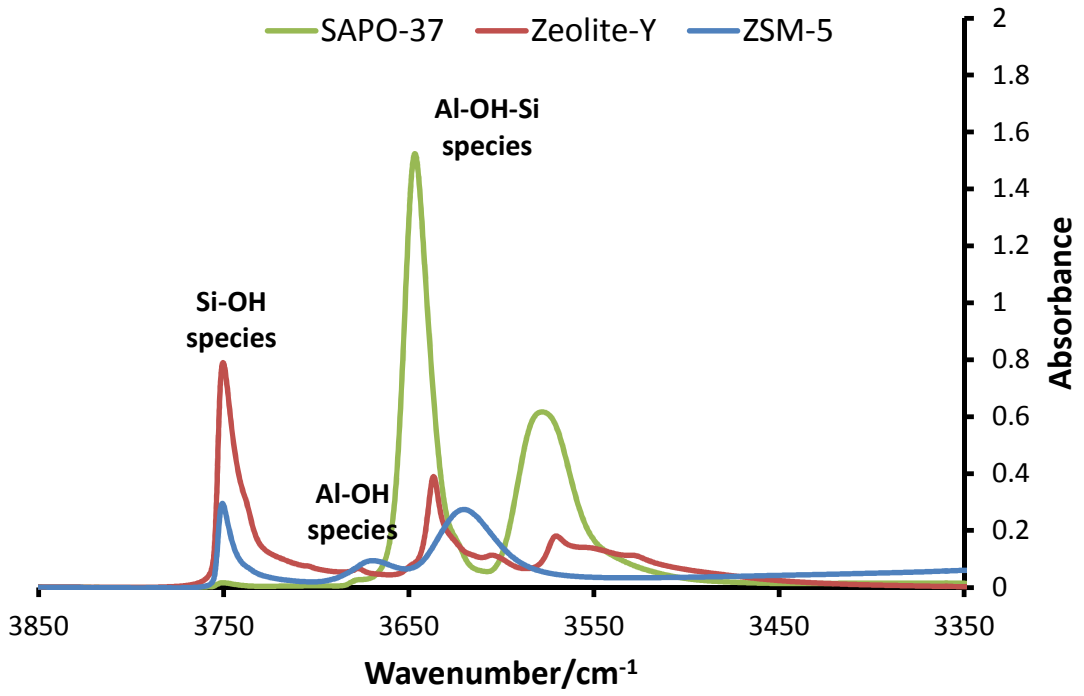

Figure S9: The background corrected FT-IR spectra of the hydroxyl region showing defect species (Si-OH and Al-OH) notably in Zeolite-Y (red) and ZSM-5 (blue) with predominant Brønsted acid sites (Si-OH-Al) in SAPO-37 (green) before adsorption of probe molecules.

Low-temperature CO FT-IR data

Table S4: Summary of low-temperature CO FT-IR data.

Sample	Before CO/cm^{-1}	After CO/cm^{-1}	Shift/cm^{-1}	Before CO/cm^{-1}	After CO/cm^{-1}	Shift/cm^{-1}	CO area/au
SAPO-37	3647*	3342	305	N/A	N/A	N/A	0.854
FAU	3636	3269	367	3601	3190	411	0.272
ZSM-5	3616	3291	328	3669	3467	202	0.663

*The band at 3575 cm^{-1} for SAPO-37 is not considered as this shows no interaction with CO

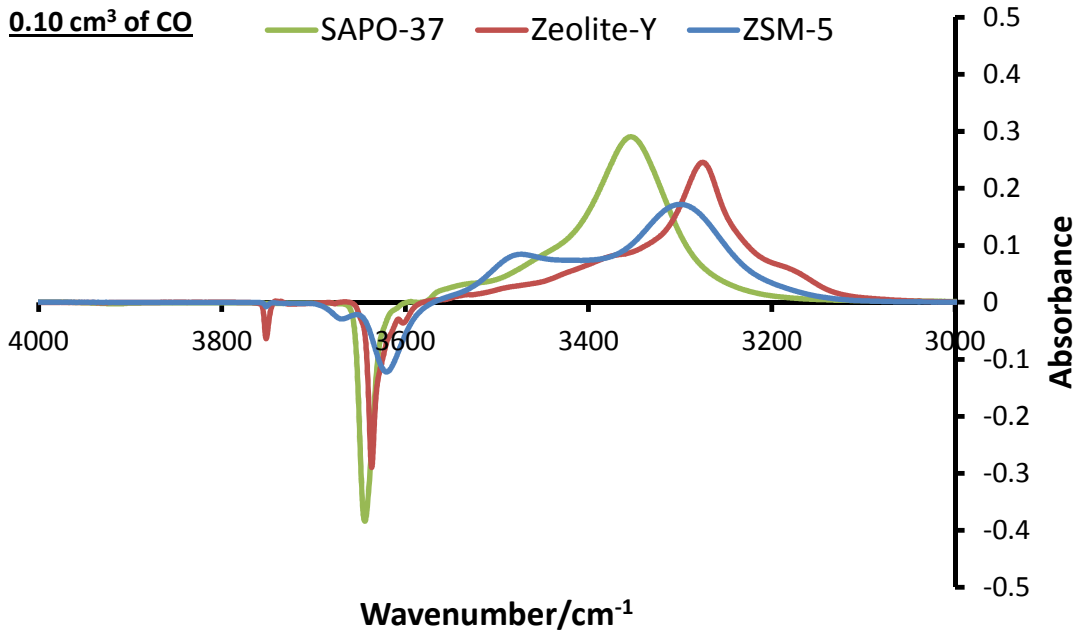

Figure S10: Hydroxyl region of zeotype materials on adsorbing 0.10 cm^3 of CO, showing CO adsorption on Si-OH-Al species and Si-OH with new peaks appearing corresponding to O-H--CO interactions.

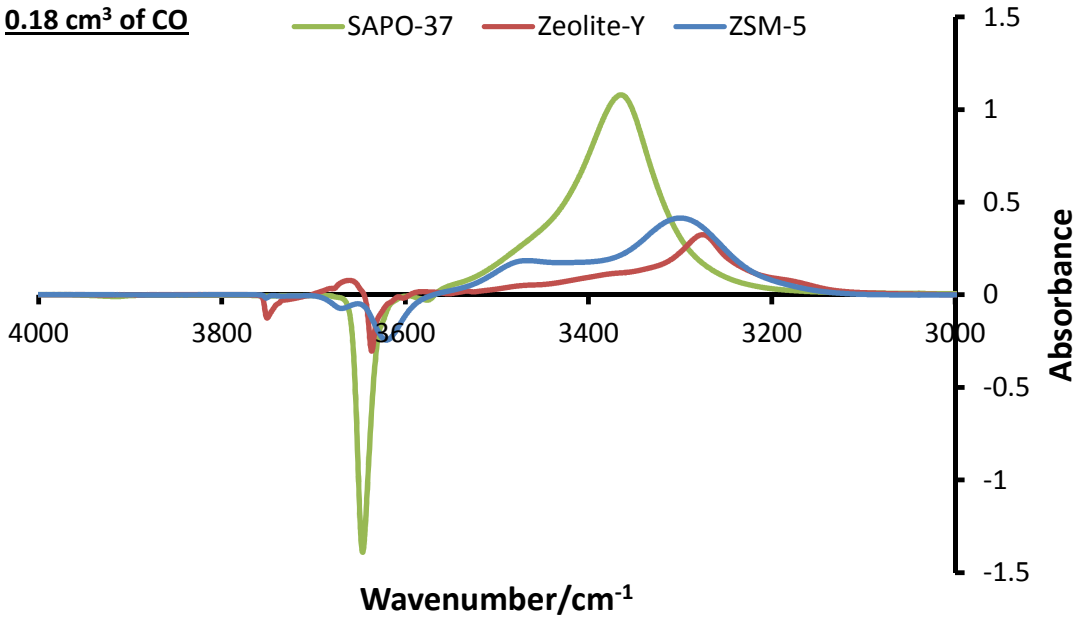

Figure S11: Hydroxyl region of zeotype materials on adsorbing 0.18 cm^3 of CO, showing CO adsorption on Si-OH-Al species and Si-OH with new peaks appearing corresponding to O-H--CO interactions.

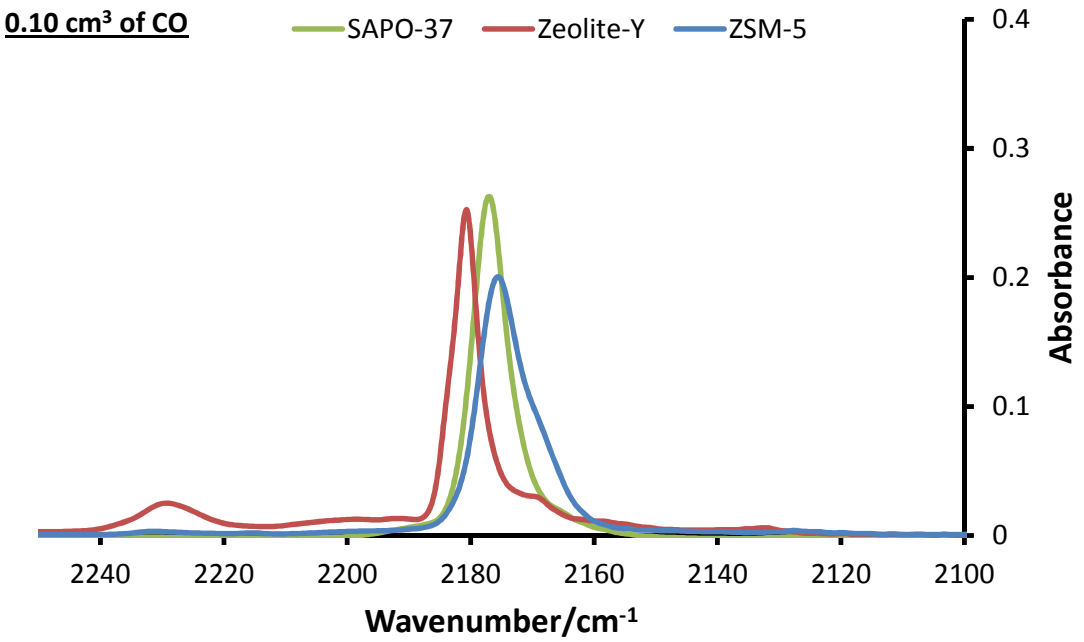

Figure S12: CO region of zeotype materials on adsorbing 0.10 cm^3 of CO, indicating Brønsted acid sites (2185 – 2170 cm^{-1}), Lewis acid sites (2200 cm^{-1}) and strong Lewis acid sites (2230 cm^{-1}).

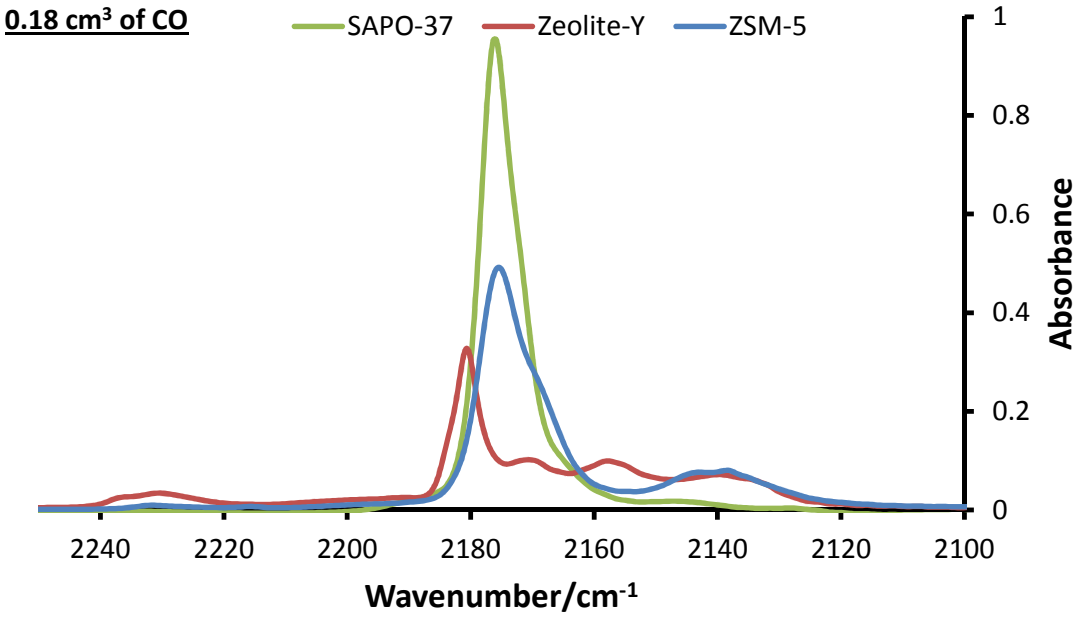

Figure S13: CO region of zeotype materials on adsorbing 0.18 cm^3 of CO, indicating Brønsted acid sites (2185 – 2170 cm^{-1}), Lewis acid sites (2200 cm^{-1}) and strong Lewis acid sites (2230 cm^{-1}).

Collidine-probed FT-IR data

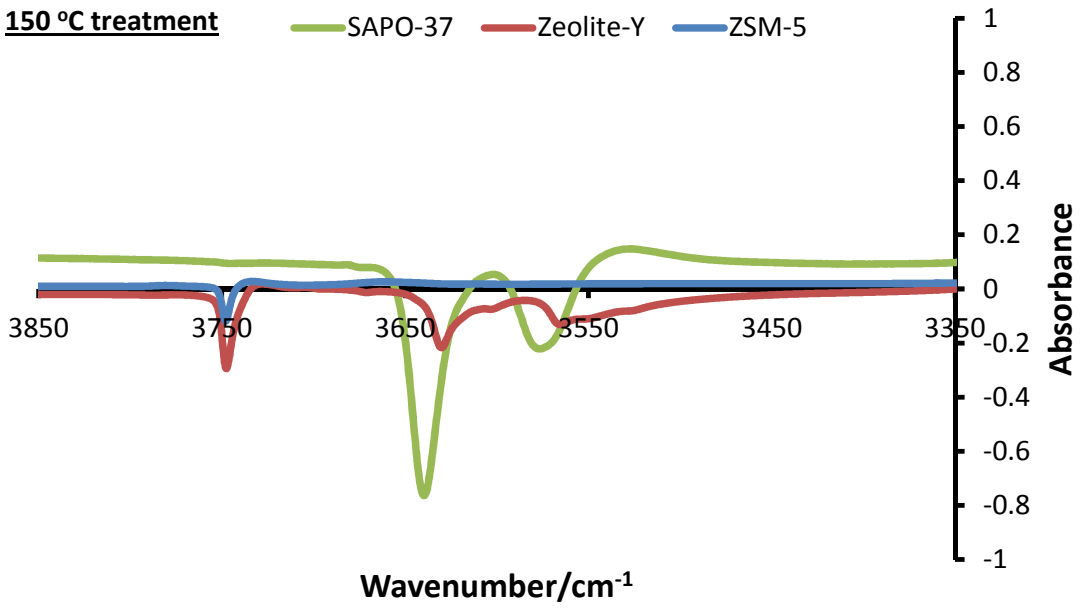

Figure S14: Collidine-probed FT-IR spectra of the hydroxyl region, after treatment at 150 °C for SAPO-37 (green), Zeolite-Y (red) and ZSM-5 (blue).

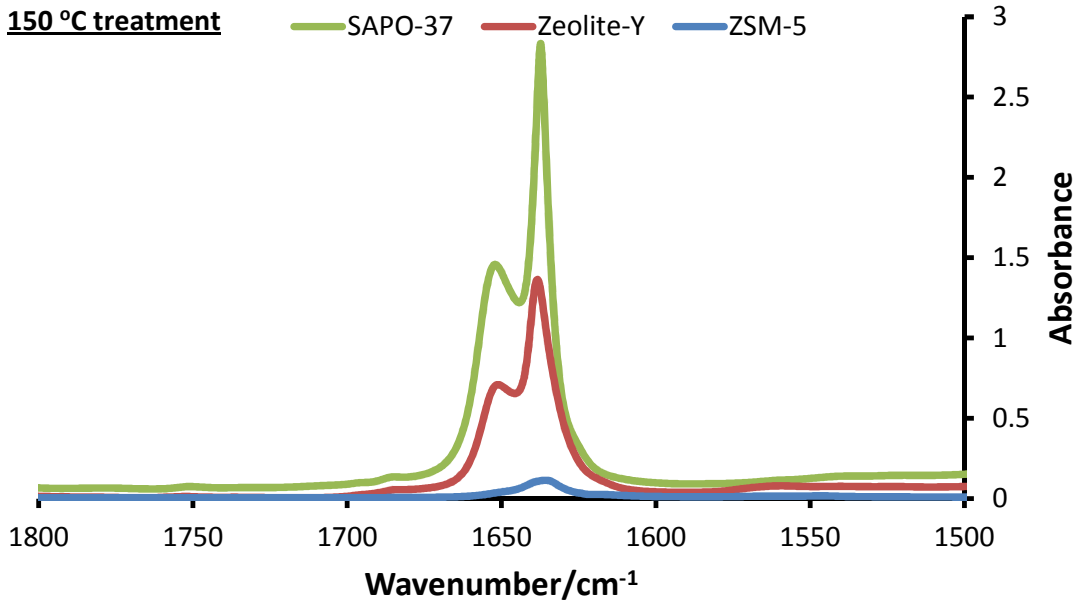

Figure S15: Collidine-probed FT-IR spectra of the C-C stretching region, after treatment at 150 °C for SAPO-37 (green), Zeolite-Y (red) and ZSM-5 (blue).

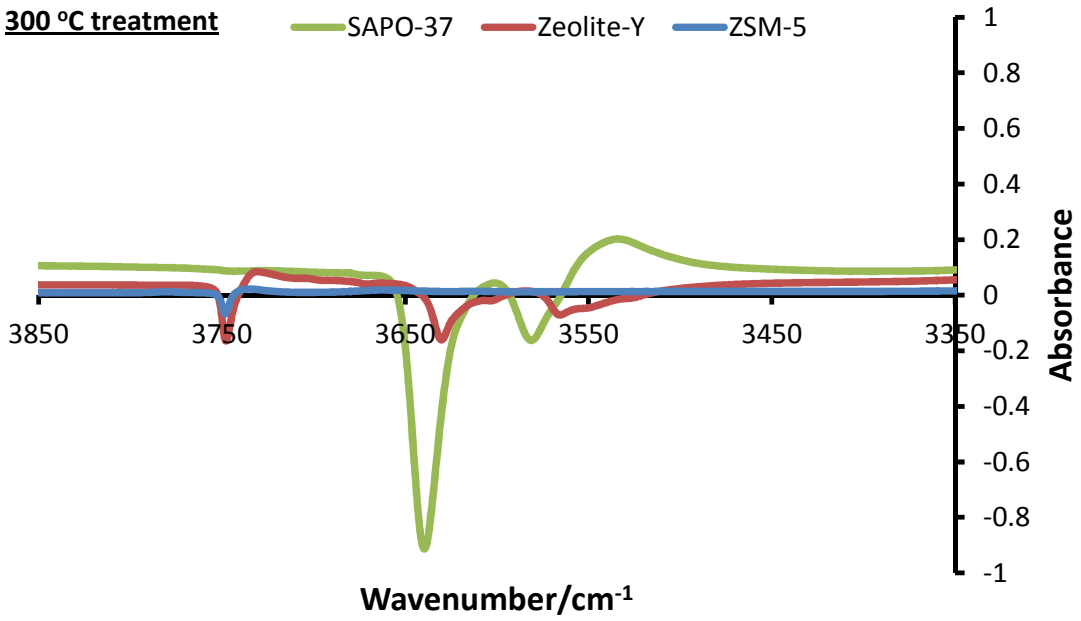

Figure S16: Collidine-probed FT-IR spectra of the hydroxyl region, after treatment at 300 °C for SAPO-37 (green), Zeolite-Y (red) and ZSM-5 (blue).

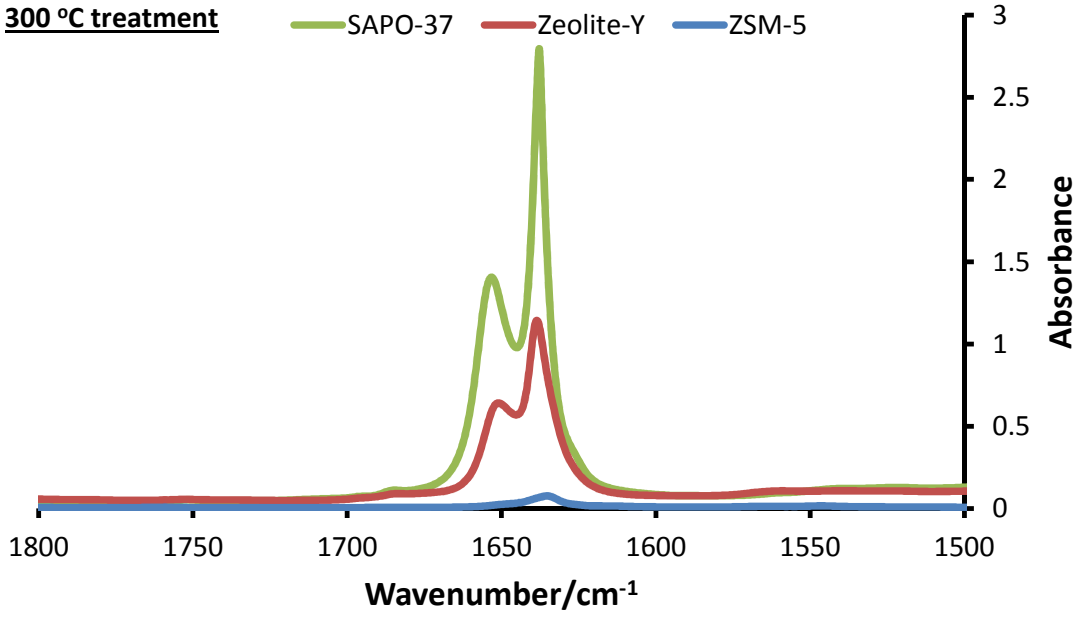

Figure S17: Collidine-probed FT-IR spectra of the C-C stretching region, after treatment at 300 °C for SAPO-37 (green), Zeolite-Y (red) and ZSM-5 (blue).

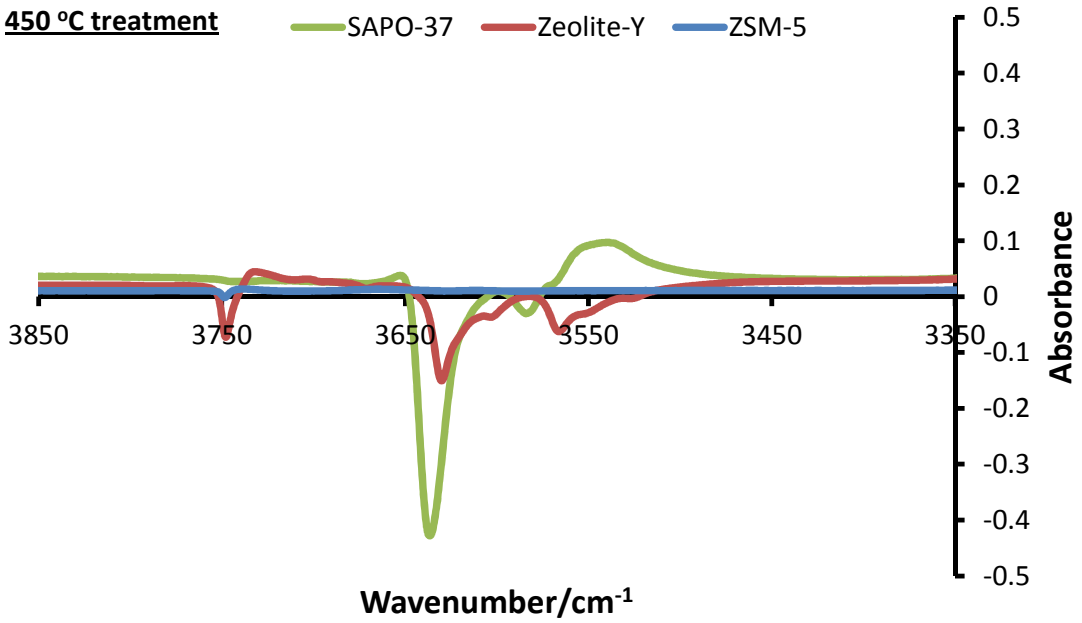

Figure S18: Collidine-probed FT-IR spectra of the hydroxyl region, after treatment at 450 °C for SAPO-37 (green), Zeolite-Y (red) and ZSM-5 (blue).

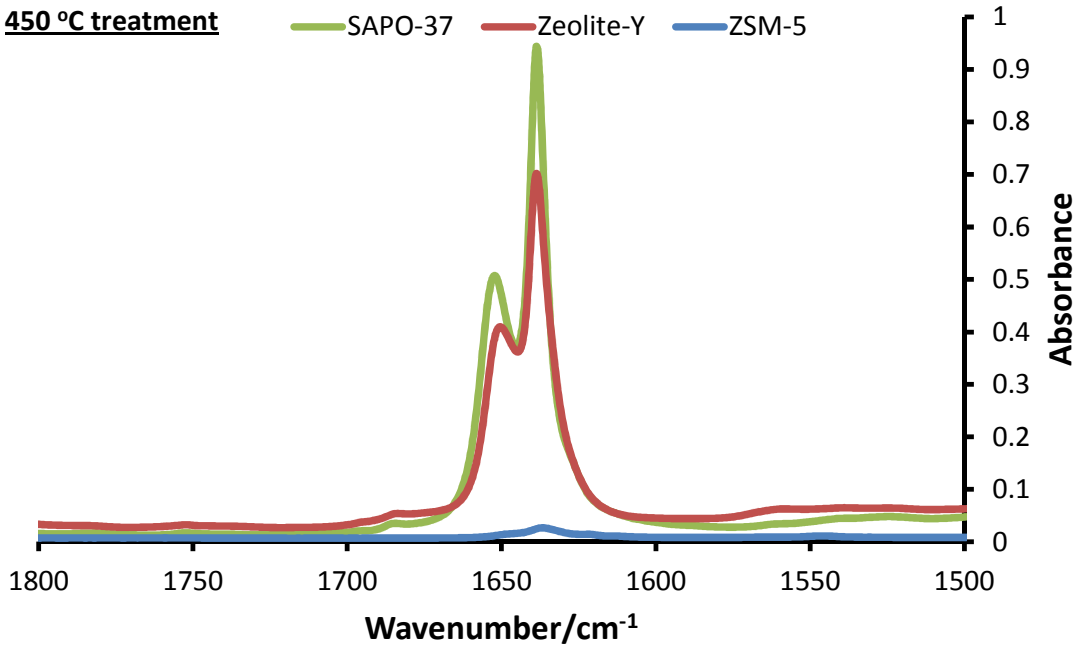

Figure S19: Collidine-probed FT-IR spectra of the C-C stretching region, after treatment at 450 °C for SAPO-37 (green), Zeolite-Y (red) and ZSM-5 (blue).

Quantification of collidine peak areas to number of acidic sites

Emeis showed that:[8]

$$\text{Moles} = IA \times \pi R^2 / IMEC$$

where Moles is moles of pyridinium adsorbed on the sample (in µmol). IA is the integrated area (in cm^{-1}) of the pyridinium peak at 1545 cm^{-1}, R is the radius of the FT-IR pellet (in cm) and IMEC is the integrated molar extinction coefficient (in cm μmol^{-1}) for the 1545 cm^{-1} pyridinium peak, found to be 1.67 cm μmol^{-1} by Emeis.[8]

Gora-Marek *et al* shows that the relationship of the molar extinction coefficient pyridinium ion (at 1545 cm^{-1}) to the collidine ion (at 1637 cm^{-1}) is 0.06 cm^2 μmol^{-1} to 0.62 cm^2 μmol^{-1}.[9]

As such the integrated molar extinction coefficient for collidine can be estimated as:

1.67 cm μmol^{-1} x (0.62 cm^2 μmol^{-1})/(0.06 cm^2 μmol^{-1}) = 17.26 cm μmol^{-1}

In our experiments, we used discs of 1.3 cm diameter; therefore, R takes the value of 0.65 cm.

This gives the relationship that:

Moles = IA x (0.0769 cm µmol)

The area total area of the collidine peak at 1637 cm^{-1} via FT-IR value for SAPO-37 is 5.367 cm^{-1} mg^{-1}.

As such the moles of collidine are:

5.367 cm^{-1} mg^{-1} x (0.0769 cm µmol) = 0.413 µmol mg^{-1} = 0.413 mmol g^{-1}

Table S5: Comparison of total acidity from collidine FT-IR, NH_3-TPD and predicted acid site from dopant loading (ICP).

Sample	Total acidity/(mmol/g)		
	Collidine FT-IR[a]	NH_3-TPD[b]	Dopant loading[c]
SAPO-37	0.41	0.93	1.05
FAU	0.21	0.33	1.06
ZSM-5	0.02	0.55	1.10

a) Derived from the total area of collidine multiplied by 0.0769 (cm µmol). b) Taken directly from NH_3-TPD data. c) Calculated assuming one mole of Si generates one mole of acid sites in SAPO-37, or one mole of Al generates one mole of acid sites in Zeolite-Y and ZSM-5, data from Table S1.

Post-catalysis characterisation data

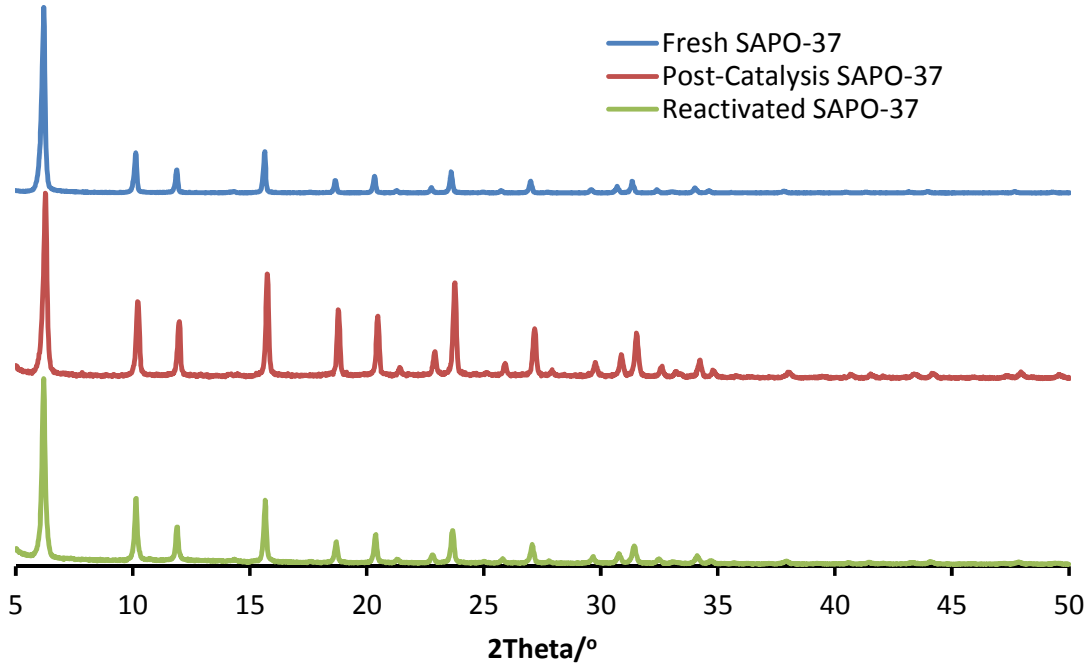

Figure S20: Contrasting powder XRD patterns of Fresh SAPO-37, Post-Catalysis SAPO-37 and reactivated SAPO-37 showing the sample is still phase pure and crystalline on reactivation.

Table S6: Total pore volumes of SAPO-37 species estimated from N_2 physisorption isotherms, before catalysis, after catalysis and on reactivation. Showing pore volume is recovered on reactivation.

System	Total pore volume/$cm^3\ g^{-1}$	Micropore volume/$cm^3\ g^{-1}$
Fresh Virgin SAPO-37[a]	0.045	0.010
Post-Catalysis SAPO-37[b]	0.017	0.001
Reactivated SAPO-37[c]	0.036	0.011

a) Activated, pre-catalysis. b) Post-catalysis SAPO-37 had been dried, but not calcined. c) Post-catalysis SAPO-37 after recalcination, reactivated.

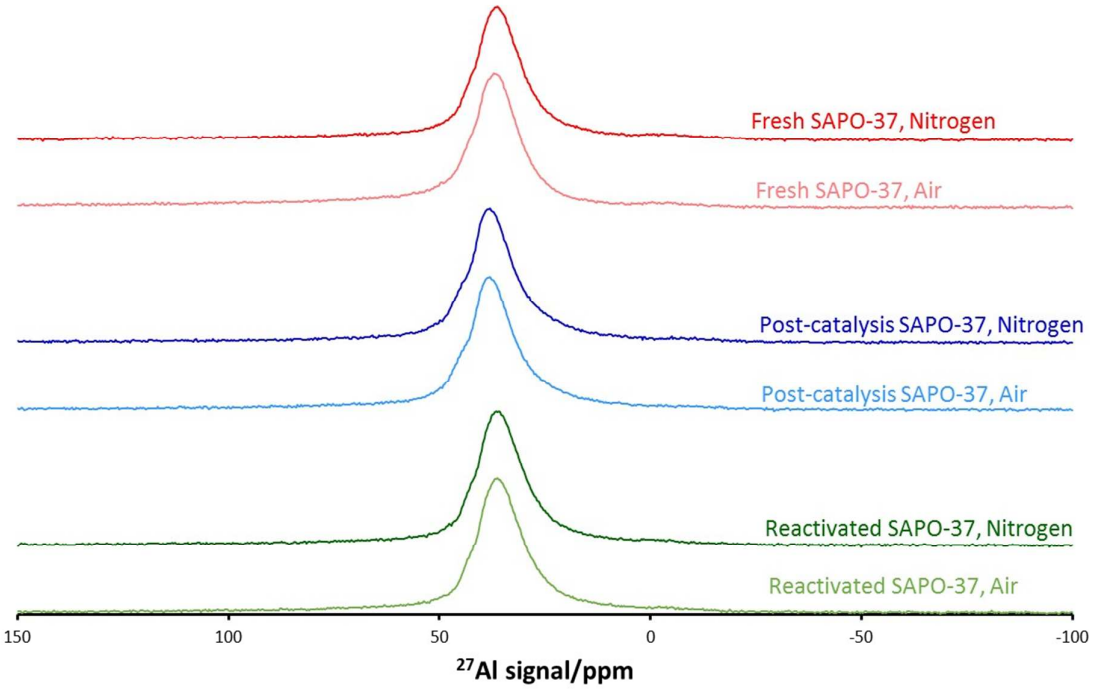

Figure S21: 1D ^{27}Al MAS NMR of Fresh SAPO-37, Post-Catalysis SAPO-37 and reactivated SAPO-37, performed under nitrogen and under air, after 12 hours of exposure to air. The spectra are near identical showing no change in the structural integrity of the sample.

References

1) Levy, A. B.; Raja, R.; Potter, M. E. *US Patent* US 9,221,762, **2015**.
2) Fung, B. M.; Khitrin, A. K.; Ermolaev K. *J. Magn. Reson*. **2000**, *142*, 97-101.
3) Amoureux, J. P.; Fernandez, C.; Steuernagel, S. *J. Magn. Reson.* **1996**, *123*, 116-118.
4) van Beek, J. D. *J. Magn. Reson.* **2007**, *187*, 19-26.
5) Jobic, H.; Theodorou, D. N. *Micorpor. Mesopor. Mater.* **2007**, *102*, 21-50.
6) Chudley, C.; Elliott, R. *Proc. Phys. Soc.* **1961**, *77*, 353-361.
7) Jobic, H.; Tuel, A.; Krossner, M.; Sauer, J. *J. Phys. Chem.* **1996**, *100*, 19545-19550.
8) Emies, C. A. *J. Catal.* **1993**, *141*, 347-354.
9) Gora-Marek, K.; Tarach, K.; Choi, M. *J. Phys. Chem. C* **2014**, *118*, 12266-12274.